REVIEWS

SCIENCE CHINA Materials

mater.scichina.com link.springer.com

Published online 10 August 2018 | https://doi.org/10.1007/s40843-018-9314-5

Sci China Mater 2019, 62(1): 8–24

Copper chalcogenide thermoelectric materials

Tian-Ran Wei[1], Yuting Qin[1,2], Tingting Deng[1,2], Qingfeng Song[1,2], Binbin Jiang[1,2], Ruiheng Liu[1], Pengfei Qiu[1], Xun Shi[1*] and Lidong Chen[1]

ABSTRACT Cu-based chalcogenides have received increasing attention as promising thermoelectric materials due to their high efficiency, tunable transport properties, high elemental abundance and low toxicity. In this review, we summarize the recent research progress on this large family compounds covering diamond-like chalcogenides and liquid-like Cu_2X (X=S, Se, Te) binary compounds as well as their multinary derivatives. These materials have the general features of two sublattices to decouple electron and phonon transport properties. On the one hand, the complex crystal structure and the disordered or even liquid-like sublattice bring about an intrinsically low lattice thermal conductivity. On the other hand, the rigid sublattice constitutes the charge-transport network, maintaining a decent electrical performance. For specific material systems, we demonstrate their unique structural features and outline the structure-performance correlation. Various design strategies including doping, alloying, band engineering and nanostructure architecture, covering nearly all the material scale, are also presented. Finally, the potential of the application of Cu-based chalcogenides as high-performance thermoelectric materials is briefly discussed from material design to device development.

Keywords: thermoelectric, Cu-based chalcogenides, sublattice, transport properties

INTRODUCTION

Thermoelectric materials can realize the direct conversion between heat and electricity, intriguing widespread interests in the situation of aggravating environment and energy crisis [1,2]. The performance of thermoelectric materials is usually evaluated by the dimensionless figure of merit (zT), defined as $zT = S^2\sigma T/\kappa$, where S is the Seebeck coefficient, σ is the electrical conductivity, κ is the thermal conductivity and T is the absolute temperature. These transport parameters are strongly correlated to each other, and it is the key task to decouple transport properties for a better zT [3,4]. In the 1990s, Slack proposed the concept of "phonon-glass electron-crystal" (PGEC) [5], that is, a high-performance thermoelectric material should possess a certain structure that allows carriers' efficient transfer while effectively blocking phonon propagation. In accordance with this principle, a bloom of new concepts, strategies, material systems as well as processing technologies has occurred in this field during the past twenty years, enhancing zT values well beyond unity, and even above two [6–11].

For a PGEC material, the crystal structure is usually composed of two sublattices: one constitutes the electrically conducting network while the other serves as thermal blocker and sometimes also charge reservoir. By virtue of such sublattices, Cu-based chalcogenides have emerged as one of the new, promising systems with potential for power generation [12] whose zT values as a function of emerging time are shown in Fig. 1. Also considering the high abundance and trivial toxicity of copper, Cu-based chalcogenides are expected to be inexpensive and environmentally friendly candidates for thermoelectric application.

In this review, we focus on the decoupled transport properties and the structural origins in Cu-based chalcogenides, covering liquid-like materials, diamond-like compounds, layered BiCuSeO, etc. The two sublattices commonly seen in this large family will be discussed in detail, and the relationship between the structures and the decoupled transport properties will be spotlighted. For each type of Cu-based chalcogenides, latest progress will be demonstrated.

DECOUPLED TRANSPORT PROPERTIES BY TWO INDEPENDENT SUBLATTICES

For ideal thermoelectric materials with two sublattices,

[1] State Key Laboratory of High Performance Ceramics and Superfine Microstructure, Shanghai Institute of Ceramics, Chinese Academy of Sciences, Shanghai 200050, China
[2] University of Chinese Academy of Sciences, Beijing 100049, China
[*] Corresponding author (email: xshi@mail.sic.ac.cn)

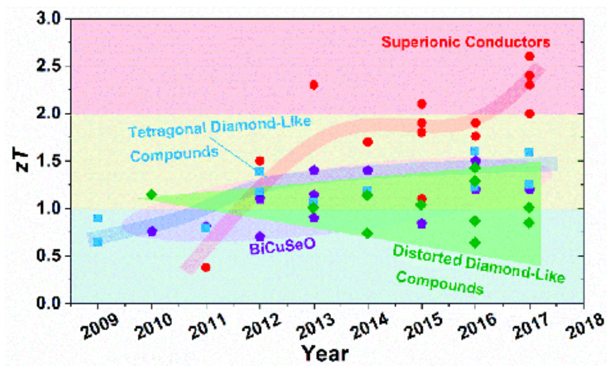

Figure 1 Timeline of zT for selected Cu-based superionic conductors [13–27] (red), tetragonal [28–37] (blue) and distorted [38–49] (green) diamond-like materials and BiCuSeO oxyselenides (purple) [50–61].

one sublattice should form a nice framework serving as carrier pathways, and the other is featured with certain disordered structures or soft bonds blocking phonon transport. Also, the features of crystal structures transform into certain band structures and phonon dispersion relations, yielding, for example, a combination of light and heavy bands that is favorable for a simultaneous realization of large Seebeck coefficient and high mobility. Certainly, the two cases in two spaces, i.e., crystal structure and band structure/phonon dispersion, are unified, thus going beyond the conventional realm of two sublattices or PGEC, offering more possibility for decoupling transport properties.

Complex/disordered sublattice and low thermal conductivity

As shown in Fig. 2a, Cu-based thermoelectric chalcogenides generally exhibit lower thermal conductivity especially at high temperatures than traditional thermoelectric materials such as SiGe and $CoSb_3$. In a simple yet intuitive way, lattice thermal conductivity is related to the heat capacity (C_V), speed of sound (v) and mean free path of phonons (l) *via* $\kappa_L = 1/3C_V vl$ [62]. Therefore κ_L can be lowered by suppressing the three parameters, which is determined by the complex or disordered crystal structures.

The mean free path of phonons, l, can be suppressed by introducing scattering centers with multiple scales. On the atomic scale, complex crystal structures featured by large unit cell or large atom number N intrinsically result in small l [63]. Basically, solids possess $3N$ vibrational modes including 3 acoustic modes and $3(N-1)$ optical modes [64]. The optical ones store most of the thermal energy, but contribute little to heat conduction because of their low group velocity. In addition, the heat-carrying acoustic modes are tend to be interacted with and hindered by the optical branches [65]. From another perspective, the cut-off frequency (or the Debye temperature) for the acoustic modes is considerably lower in these complex systems. As shown in Fig. 2b, κ_L for Cu-based chalcogenides exhibits a negative dependence on the primitive cell volume, showing that a large unit cell is a practical indicator for low thermal conductivity.

Normally, heat capacity is an inherent quality of a material, which is usually difficult to modulate. For conventional solids at room and high temperatures, C_V is close to or higher than the Dulong-Petit limit, $3Nk_B$ or $3R$ [65]. Inspiringly, the liquid-like character in Cu_2X compounds provides an effective solution to reducing C_V. As shown in Fig. 3a, Cu_2Se possesses two sublattices: the rigid FCC framework of Se atoms and the disordered and flowing sublattice of Cu. At high temperatures, Cu ions migrate from one site (interstitial one formed by Se) to another, exhibiting a flowing character that is

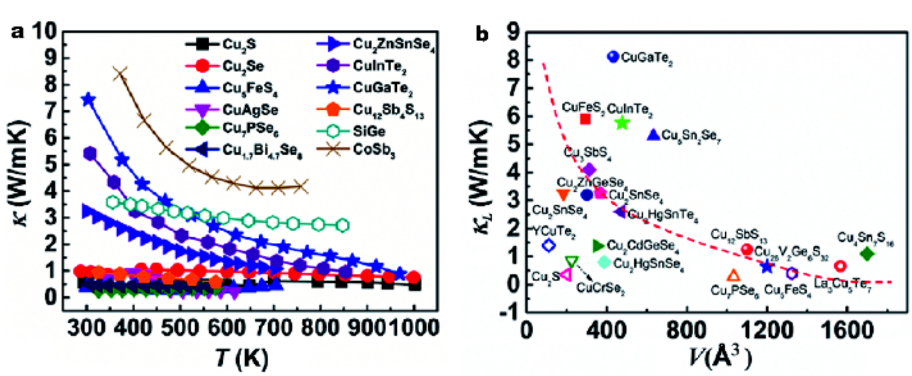

Figure 2 (a) Thermal conductivity for Cu-based chalcogenides; (b) lattice thermal conductivity as a function of the primitive cell volume in a variety of Cu-based chalcogenides at 300 K. The dashed line shows a negative correlation between the lattice thermal conductivity and the primitive cell volume. Data are taken from Refs. [14,16,29–31,42,45,66–77].

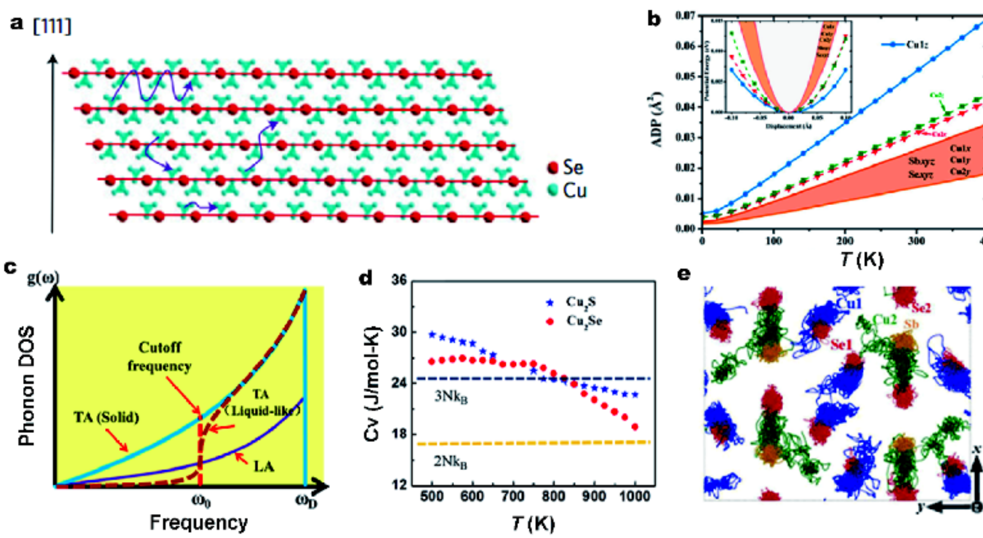

Figure 3 Liquid-like behavior in Cu-based materials. (a) Crystal structure of Cu_2Se where Cu atoms flow among the interstitial sites of Se rigid sublattice, reproduced from Ref. [14], Copyright 2012, Nature Publishing Group; (b) schematic phonon DOS for solid and liquid-like materials, adapted from Ref. [12], Copyright 2016, Elsevier; (c) temperature dependence of the specific heat in Cu_2Se and Cu_2S; (d) atomic displacement parameter varying with temperature in Cu_3SbSe_3 and (e) trajectories of atoms from molecular dynamics simulations for Cu_3SbSe_3 at 400 K , reproduced from Ref. [79,80], Copyright 2014, National Academy of Sciences and Copyright 2014, Nature Publishing Group, respectively.

analogous to liquid [14,78]. It is known that transverse modes are missing in liquid (Fig. 3b), thus yielding a limit of heat capacity of $2Nk_B$. Therefore, C_V of Cu_2Se is noticeably suppressed as shown in Fig. 3c. Similarly, a "part-crystalline part-liquid" state is proposed in Cu_3SbSe_3 [79], which is constituted by a rigid crystalline sublattice and a noncrystalline sublattice. Cu atoms vibrate in large amplitude with a high atomic displacement parameter (ADP) as shown in Fig. 3d and e, and can be regarded as a liquid state.

In fact, the structural features and dynamic behaviour of liquid-like materials and the mechanism of suppressed thermal conductivity are more complicated than we discussed above. It is experimentally confirmed by Li *et al.* [81] that the transverse acoustic phonon modes are completely suppressed by ultrafast dynamic disorder in $AgCrSe_2$. However, Voneshen *et al.* [82] argue that the fast local hops of Cu in Cu_2Se should be considered as anharmonic vibration, and the transitional diffusion of Cu is too slow to affect phonon propagation.

Low thermal conductivity can also come from lone pairs, as proposed by Skoug *et al.* [83] in nitrogen-group chalcogenides. Owing to the different delocalization behaviours of Sb 5s lone pair electrons, Cu_3SbSe_4, $CuSbSe_2$ and Cu_3SbSe_3 exhibit different Se–Sb–Se angles as shown in Fig. 4. Essentially, the mutual repulsion between the lone pair electrons and the adjacent valence electrons during thermal agitation leads to large lattice anharmonicity.

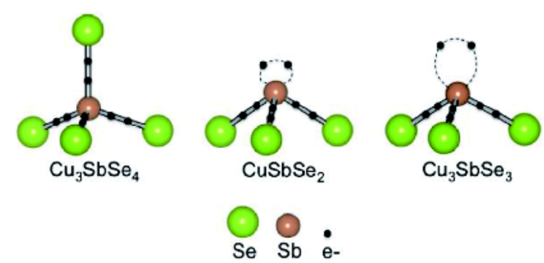

Figure 4 Schematic diagram of the lone pair electrons situation in Cu_3SbSe_4, $CuSbSe_2$, Cu_3SbSe_3 compounds, reproduced from Ref. [83], Copyright 2011, the American Physical Society.

Structural retainer and electrical transport

It is somewhat unexpected that $Cu_{2-x}Se$ liquid-like materials with such a low thermal conductivity exhibit a decent electrical conductivity [14]. Based on the first-principle calculations, Sun *et al.* [84] found that the valence band maxima (VBM) and the transport of holes are dominated by Se orbitals while Cu vacancies serve as efficient acceptors, shifting the Fermi level, but do not change the band shape.

For many multinary Cu-based compounds, the electrically conducting channel (mostly VBM) is considered to be constituted by Cu–X bonds. Taking Cu_2SnSe_3 [39] as an example in Fig. 5a, the VBM is mostly occupied by the p-d hybridization from Cu–Se bonds, acting as the

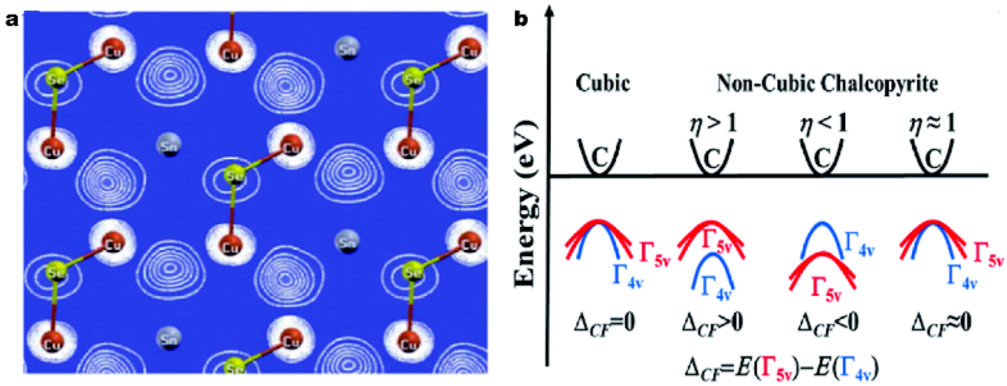

Figure 5 (a) Partial charge density of the state plots of Cu_2SnSe_3 near the upper valence-band, reproduced from Ref. [39] Copyright 2010, the American Chemical Society; (b) band convergence in the pseudocubic diamond-like chalcogenides, reproduced from Ref. [32], Copyright 2014, Wiley-VCH GmBH&Co.

structural retainer and charge conduction path. Sn orbitals contribute little to the occupied states while predominantly affect the conductive band. The Cu–X conduction network has also been proposed in BiCuSeO [85], Cu_3SbSe_4 [86], $Cu_2CdZnSe_4$ [28], etc.

Derived from the high-symmetry diamond, the diamond-like Cu chalcogenides possess highly degenerate valence bands, ensuring a large Seebeck coefficient and power factor even at a high doping level. Particularly, the power factor (PF) can be maximized by reducing the band split off, which is proposed by Zhang *et al.* [32] as a pseudocubic approach to screen and develop high-performance non-cubic materials. Specifically, the tetragonal diamond-like chalcogenides form a long-range cubic-like and short-range non-cubic structure. As shown in Fig. 5b, when the bands are degenerate, that is, the valence band splitting energy Δ_{CF} approaches zero, the distortion parameter $\eta=c/2a$ gets close to 1, leading to the maximum PF. The unity-η rule and the pseudocubic approach have been found effective in screening high-performance tetragonal diamond-like compounds [87,88], which will be discussed later.

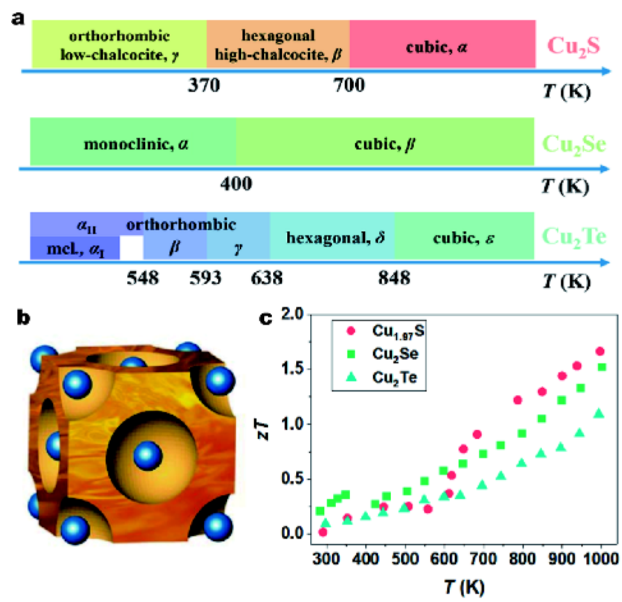

Figure 6 (a) Phases varying with temperature for Cu_2X compounds; (b) schematic depiction of high-temperature superionic crystal structure of Cu_2S, reproduced from Ref. [16], Copyright 2014, Wiley-VCH GmBH&Co. The blue spheres represent sulfur atoms, and the liquid-like copper ions (yellow) travel freely within the sulfide sublattice. (c) zT as a function of temperature for Cu_2X compounds [14,16,18].

LIQUID-LIKE OR SUPERIONIC MATERIALS

Cu_2X (X=S, Se, Te) compounds and their alloys

Liquid-like materials may be the most typical examples of using two sublattices to optimize thermoelectric properties. As discussed above, Cu_2X materials at high temperatures exhibit superionic cubic phases where Cu atoms flow through the X rigid framework (Fig. 3a and 6b). Benefiting from this "phonon-liquid electron-crystal (PLEC)" structure, this family in the pristine form shows high zT values ranging from 1.0 to 1.7 as demonstrated in Fig. 6c. The phase structures at low temperatures are quite complex for these compounds and vary with the ratio of Cu to X, and at least one phase transition occurs with increasing temperature as shown in Fig. 6a.

In 2012, Liu *et al.* [14] found the unique thermal transport behavior of $Cu_{2-x}Se$ superionic conductor and proposed the concept PLEC as an extension to PGEC. Later in 2014 Cu_2S was found to exhibit similar liquid-like

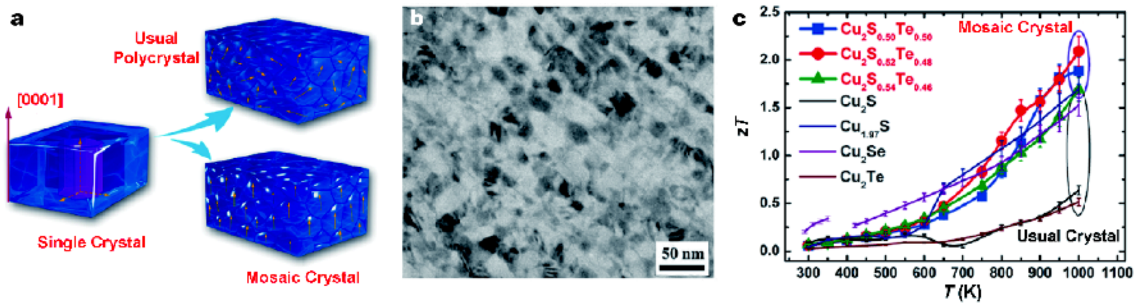

Figure 7 (a) Schematic depiction of mosaic structures, (b) TEM image for $Cu_2S_{0.5}Te_{0.5}$ as a mosaic crystal, (c) zT values for mosaic and usual crystals. Figures are adapted from Ref. [17], Copyright 2015, Wiley-VCH GmbH&Co.

behavior but with lower effective mass and higher deformation potential, showing a high zT of 1.7 at 1,000 K [16]. The phases in Cu_2Te are even more complex as shown in Fig. 6a. In 2015, He *et al.* [18] reported that $Cu_{2-x}Te$ has many stable and meta-stable phases as well as much weaker ionic bonds than $Cu_{2-x}S$ and $Cu_{2-x}Se$. Owing to the optimized carrier concentrations and lowered thermal conductivity, zT value in Cu_2Te was grossly improved from 0.55 in the SPS-ed samples to 1.1 in the directly annealed samples at 1,000 K.

Based on a simple chemical intuition [89], the increase of atomic size and mass from S to Te and the decrease of electronegativity lead to a weaker and less ionic Cu–X bond. This means that Cu vacancies are more prone to form, resulting in a higher carrier density. Meanwhile the lattice thermal conductivity is normally lower in tellurides than selenides or sulfides due to the larger Te atoms and weaker bonds. In addition, all of the three Cu_2X compounds exhibit similar disordered cubic structures at high temperatures. So alloying or forming solid solutions is likely to not only further reduce the already low thermal conductivity, but also tune the electrical transport properties.

Zhao *et al.* [90] found that Cu_2Se and Cu_2S can form a continuous solid solution over the entire composition range. The solid solutions are polymorphic materials composed of varied phases with different proportions at room temperature, and transform into single cubic phase at high temperatures. The lattice thermal conductivity was significantly lowered not only by alloy scattering of phonons but also due to the reduced sound speed. In addition, Cu–S bond is stronger than Cu–Se bond, leading to reduced amount of Cu vacancies and lower carrier concentration towards the optimal value. A maximum zT value of ~2.0 at 1,000 K was achieved in slightly S-doped Cu_2Se [23].

As for Cu_2S-Cu_2Te alloys, due to the large mass and size contrast between S and Te, a special mosaic crystal structure [17] was built in Cu_2(S, Te) bulk single-phase polycrystalline materials as shown in Fig. 7. That is, the blocks exhibit a nearly identical orientation, so the bulk appears like a single crystal from the macroscale point of view but contains a number of small-angle boundaries. The electrons are freely transferred along the frames of quasi-single crystals and phonons are strongly scattered by lattice strains or interfaces of mosaic nanograins. When compared with the usual polycrystalline matrix Cu_2S or Cu_2Te, a simultaneous optimization of thermal conductivity and power factor were achieved, yielding a high zT of ~2.1 at 1,000 K, which goes beyond the traditional approaches using single crystals or nano-materials. The mosaic structures were also found in triple $Cu_{2-y}S_{1/3}Se_{1/3}Te_{1/3}$ solid solutions [91], and are considered to open a new window of realizing ultrahigh thermoelectric performance [92].

Studies on Cu_2X liquid-like materials have also been extended to nanostructured composites. By utilizing the special interaction between metal Cu and multi-walled carbon nanotubes (CNTs), Nunna *et al.* [21] realized the *in-situ* growth of Cu_2Se on the surface of CNTs and then fabricated a series of Cu_2Se/CNTs hybrid materials. Due to the high-degree homogeneously dispersed molecular CNTs inside the Cu_2Se matrix, a zT of 2.4 at 1,000 K has been achieved. Olvera *et al.* [22] reported a record zT of 2.6 at 850 K in Cu_2Se-$CuInSe_2$ composites. It was suggested that the incorporation of a small fraction of In into the Cu_2Se lattice induced partial localization of Cu^+ ions, and a hybrid structure with same Se lattice was formed. This led to a simultaneous increase in the carrier mobility and a drastic reduction in the lattice thermal conductivity. Ge *et al.* [93] prepared nanostructured $Cu_{1.8}S$ (Cu_9S_5) by mechanical alloying. By doping Na at the interstitial sites, the carrier concentration was reduced to the optimal range, and nano pores were introduced

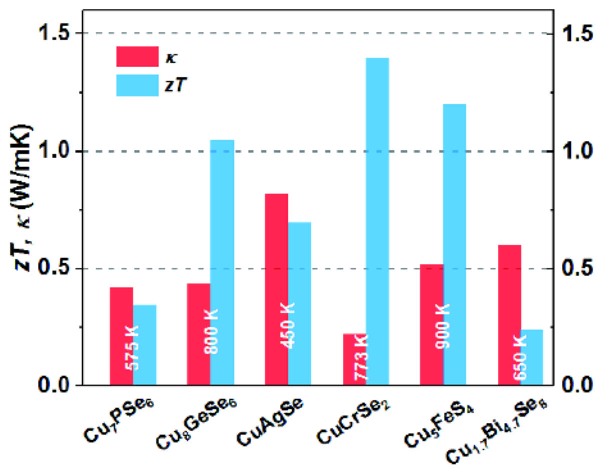

Figure 8 Thermal conductivity and maximum zT for selected ternary superionic conductors: Cu_7PSe_6 [68], $Cu_{7.6}Ag_{0.4}GeSe_{5.1}Te_{0.9}$ [94], $CuAgSe_{0.95}Te_{0.05}$ [95], $CuCrSe_2$-$AgCrSe_2$ [96], $0.8Cu_8S_4$-$0.2Cu_5FeS_4$ [67] and $Cu_{1.7}Bi_{4.7}Se_8$ [97].

resulting in suppressed thermal conductivity. A high zT of 1.1 was obtained at a relatively low temperature of 773 K.

Ternary derivatives of Cu_2X

Besides the binary Cu_2X (X = S, Se, Te) compounds, there are many derivatives which also demonstrate superionic conduction with liquid-like behavior. High-temperature thermal conductivities and maximal zT values of typical materials are summarized in Fig. 8.

CuAgSe can be regarded as an alloy between Cu_2Se and Ag_2Se. Similarly, it undergoes a structural phase transition around 480 K. Owing to the superior carrier mobility [98] and the low lattice thermal conductivity, CuAgSe behaves as a potential thermoelectric material. Stoichiometric CuAgSe shows n-type conduction, but an n-to-p transition is observed when increasing temperature in the samples with slight deficiencies of Ag or Cu [66]. By doping Te at Se site, the thermal conductivity was significantly reduced, resulting in a zT=0.7 at 450 K in $CuAgSe_{0.95}Te_{0.05}$ [66,95].

In $CuCrSe_2$, the $CrSe_2^-$ layer distributes regularly and the Cu ions occupy the interlayer space and become disordered due to the migration from one to another tetrahedral site. zT around unity at 773 K was reported [70], and an even higher zT=1.4 was claimed in $AgCrSe_2$-$CuCrSe_2$ nanocomposites by virtue of all-wavelength phonon scattering [96]. The isostructural $CuCrS_2$ exhibits a much lower zT value of 0.15 at 673 K, mainly due to the larger band gap and deteriorated electrical performance [99].

Sulfide bornite Cu_5FeS_4, a widespread natural mineral, can be regarded as a Fe- and vacancy-doped derivative of Cu_2S. This compound exhibits three phases at different temperatures as shown in Fig. 9a. The S framework provides a good electrical transport and the disordered occupation of Cu, S and the vacancies suppressed the transport of the phonons, leading to a high zT of 1.2 at 900 K in $0.8Cu_8S_4$–$0.2Cu_5Fe\square_2S_4$ ($\square$ represents a vacancy) [67]. Particularly, Cu migration was effectively hampered in the solid solution of Cu_5FeS_4-Cu_2S in comparing with Cu_2S due to the pinning effect from Fe atoms.

There are even more complex superionic derivatives. Argyrodite compounds possess a general chemical formula $A^{x+}_{12-y/x}B^{y+}Q^{2-}_6$, (A = Li^+, Cu^+, Ag^+; B = Ga^{3+}, Si^{4+}, Ge^{4+}, Sn^{4+}, P^{5+}, As^{5+}) [68,94,100]. In addition to the disordered Cu sublattice at high temperatures as shown in Fig. 10a and b, Cu_7PSe_6 and Cu_8GeSe_6 possess extremely low lattice thermal conductivity of

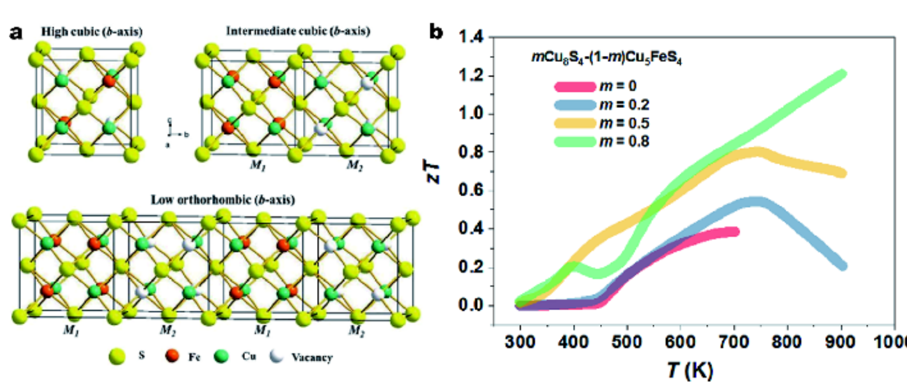

Figure 9 (a) The crystal structures of Cu_5FeS_4 for the low temperature phase and high temperature phase. Reproduced from Ref. [67], Copyright 2014, the Royal Society of Chemistry; (b) Temperature dependence for the zT value for the mCu_8S_4–$(1-m)$ Cu_5FeS_4 compound.

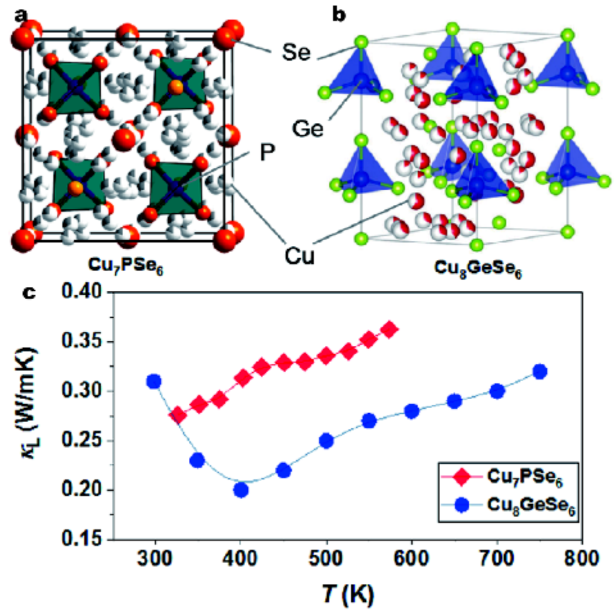

Figure 10 High-temperature crystal structure for (a) Cu_7PSe_6 (reproduced from Ref. [68], Copyright 2014, the American Chemical Society) and (b) Cu_8GeSe_6 (reproduced from Ref. [94], Copyright 2017, the Royal Society of Chemistry); (c) lattice thermal conductivity as a function of the temperature for the two compounds [68,94].

~0.3 W m^{-1} K^{-1} even at around room temperature (Fig. 10c). This is probably related to as many as 56 and 90 atoms per unit cell for the two compounds, respectively, where the low-frequency optical phonons make a difference by either trapping heat or interacting with acoustic phonons. By alloying with Ag and Te, the electrical conductivity of Cu_8GeSe_6 is greatly enhanced and the low lattice thermal conductivity is maintained, leading to a high zT of unity at 800 K [94].

Concerns about Cu migration and materials stability

The migration of Cu in liquid-like materials brings about the ultralow thermal conductivity and high zT values, but at the same time, raises widespread concerns on Cu precipitation and materials degradation. This phenomenon was clearly reported in Cu_2S by Miyatani *et al.* [101] in 1953 for the first time, and was also found within Cu_2Se by Ema [102] in 1990.

For the purpose of device application, great efforts have been made to suppress Cu drift in Cu_2X materials. It is desirable that the long-range ionic migration is suppressed while the short-range drift is maintained. For materials designing, foreign atoms [22,103] were added into the matrix with the intention to block the motion of Cu ions. The effect is observable but not considerable. The ternary Cu_5FeS_4 can be regarded as Fe- and vacancy-co-doped Cu_2S, and the migration of Cu was significantly hampered by the immobile Fe [67]. Most recently, we have studied the mechanism of Cu migration in liquid-like materials and found it is possible to greatly improve material's stability by introducing electronically-conducting but ion-blocking barriers [104]. Similarly, Tang *et al.* [105] found that the incorporated graphene three dimensional (3D) network can provide another possibility to block the migration of Cu ions and to enhance the stability of Cu_2S.

DIAMOND-LIKE Cu-BASED CHALCOGENIDES

Diamond-like compounds are a big family structurally derived from IV elementary substance, covering binary II-VI and III-V compounds, ternary I-III-VI_2 and II-IV-V_2 chalcopyrites, I_3-V-VI_4 stannites, quaternary I_2-II-IV-VI_4 compounds, and even large-cell $Cu_{12}Sb_4S_{13}$ tetrahedrites and $Cu_{26}V_2M_6S_{32}$ (M=As, Ge, Sn, Sb) colusites. The diverse interatomic distances cation–X and the difference in electronegativity between the cations result in a natural superlattice structure. For nearly all the p-type semiconductors in this family, Cu–X constitutes VBM for the conduction of hole carriers while other cation atoms bond with X contributing to CBM.

Tetragonal diamond-like compounds

The tetragonal diamond-like compounds are composed of two cubic zinc-blended structure units, including I-III-VI_2, I_3-V-VI_4 and I_2-II-IV-VI_4 compounds as shown in Fig. 11. The crystal structures, band gaps and zT values for selected materials are displayed in Table 1.

Ternary I-III-VI_2 compounds can be regarded as the super cell of the zinc-blend structure as shown in Fig. 11. High zT values of 1.18 and 1.4 were realized in $CuInTe_2$ [30] and $CuGaTe_2$ [31], respectively, being the highest ones among diamond-like compounds. While ternary $CuFeS_2$, namely chalcopyrite, an important natural copper ore, is one of the few n-type materials among the Cu-based diamond-like thermoelectric materials, which is attributed to the sulfur vacancies. Maximum zT values around 0.25 were reported for this material [74,111]. However, further enhancement of thermoelectric performance in $CuFeS_2$ is hindered by the low carrier mobility that is dominated by localized d electrons of Fe.

I_3-V-VI_4 compounds can be regarded as four-fold of ZnSe structure. Among them, Cu_3SbSe_4 with a narrow band gap of ~0.3 eV is a also promising candidate

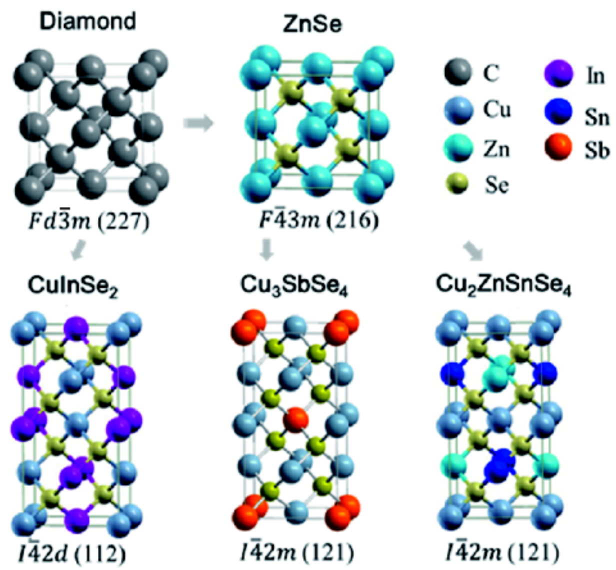

Figure 11 Crystal structure of diamond, zinc-blende ZnSe, chalcopyrite $CuInSe_2$, stannite Cu_3SbSe_4 and $Cu_2ZnSnSe_4$.

Table 1 Space group, band gap and zT for selected I-III-VI_2, I_3-V-VI_4 and I_2-II-IV-VI_4 tetragonal diamond-like compounds

Chemical formula	Space group	E_g (eV)	zT, T (K)	Ref.
$CuGaTe_2$	I-42d	1.2	1.4, 923	[31]
$CuInTe_2$	I-42d	1.02	1.18, 850	[30]
$CuFeS_2$ (n)	I-42d	0.34	0.21, 573	[74]
Cu_3SbSe_4	I-42m	0.31	1.26, 673	[35]
Cu_3SbS_4	I-42m	0.9	0.10, 300	[73]
$Cu_2CdSnSe_4$	I-42m	0.98	0.65, 700	[28]
$Cu_2ZnSnSe_4$	I-42m	1.41	0.95, 850	[29]
$Cu_2HgSnSe_4$	I-42m	1.81	0.2, 723	[71]
$Cu_2HgGeSe_4$	I-42m	/	0.34, 733	[106]
$Cu_2HgSnTe_4$	I-42m	1.62	/	[107]
$Cu_2MgSnSe_4$	I-42m	1.7	0.42, 700	[108]
$Cu_2CdGeSe_4$	I-42m	1.2	0.42, 723	[72]
$Cu_2ZnGeSe_4$	I-42m	1.4	0.55, 723	[109]
Cu_2ZnGeS_4	I-42m	1.5	/	[110]

[35,36,112,113]. Quaternary I_2-II-IV-VI_4 (I=Cu; II=Zn, Cd, Fe, Co, Mn, Hg, Mg; IV=Ge, Sn; VI=S, Se, Te) compounds generally exhibit a larger band gap and lower mobility than the ternary counterparts, which is likely due to the localized d-orbitals of the transition metal elements.

The generally low carrier concentrations as well as the high lattice thermal conductivity in the pristine form especially in the low and medium temperature range may be the common disadvantages for these tetragonal diamond-like chalcogenides. Doping was widely employed to improve the carrier concentration and the electrical conductivity, such as $CuIn(Ga)_{1-x}M_xTe_2$ (M=Zn, Mn, Cd, Hg, Ni, Ag, Gd) [114–118], $Cu_{1-x}Fe_{1+x}S_2$ [119], $Cu_3Sb_{1-x}M_xSe_4$ (M=Al, In, Sn, Ge, Bi) [35,120–122] and $Cu_2Cd_{1-x}In_xSnSe_4$ [123]. Introducing vacancies is another practical way for the electrical transport optimization as well as the lattice thermal conductivity minimizing. Cu vacancy is the most common for p-type doping such as $Cu_{1-x}In(Ga)Te_2$ [87,124] and $Cu_{3-x}SbSe_4$ [125], which is due to the small formation energy of this defect, while anion vacancies are feasible for donor doping as seen in $CuFeS_{2-x}$ [74] and Cu_2FeSnS_{4-x} [126].

The pseudocubic approach has been testified in several compounds such as $CuGaTe_2$ [87], Cu_2MGeSe_4 [127] and $Cu_2TMSnSe_4$ (TM=Mn, Fe, Co) [88]. The distortion parameter, η, as a function of the cell parameter a for the tetragonal diamond-like chalcogenides is shown in Fig. 12a. It can be qualitatively utilized as an indicator map to discover or optimize high-performance tetragonal dia-

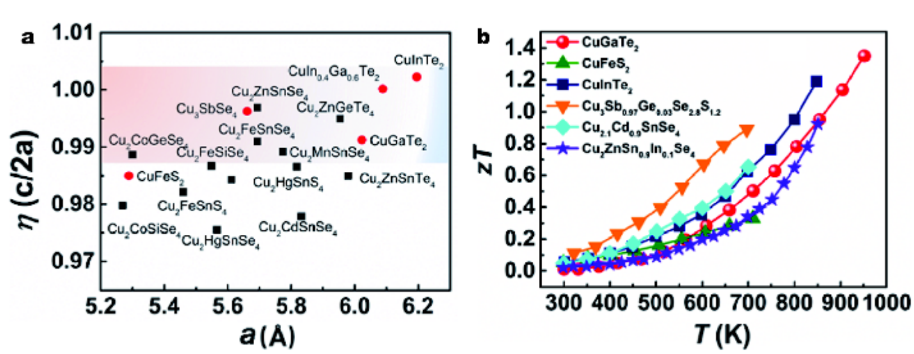

Figure 12 (a) Distortion parameter as a function of the lattice parameter a [28,72,87,106–108,119,123,126,136,137]. (b) Temperature dependence of zT for tetragonal diamond-like compounds [28,29,87,112,119].

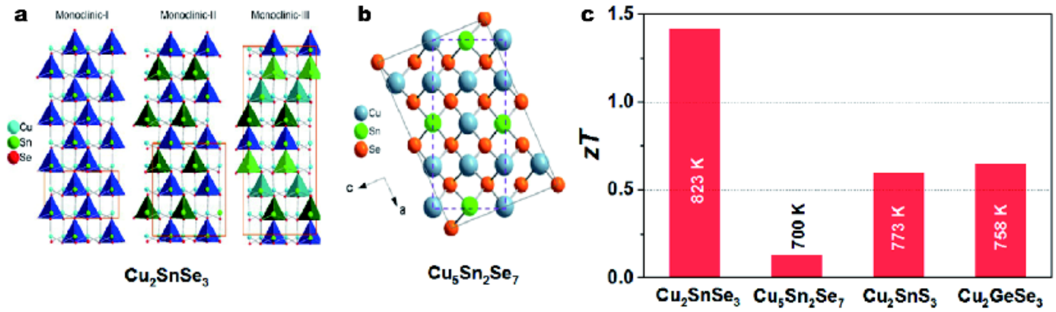

Figure 13 Crystal structure of (a) Cu_2SnSe_3 (reproduced from Ref. [140], Copyright 2013, the American Chemical Society) and (b) $Cu_5Sn_2Se_7$ (reproduced from Ref. [141], Copyright 2014, the American Chemical Society); (c) zT of distorted diamond-like Cu_2SnSe_3 [38], $Cu_5Sn_2Se_7$ [141], Cu_2SnS_3 [142] and Cu_2GeSe_3 [143].

mond-like thermoelectric materials, which can be confirmed by the thermoelectric performance of the reported diamond-like compounds as shown in Fig. 12b.

For thermal conduction suppression, alloying is an effective approach *via* intensifying phonon scattering by mass and strain fluctuations [128] as demonstrated in several solid solutions, such as $CuGa_{1-x}In_xTe_2$ [129], $Cu_3SbSe_{4-x}S_x$ [36,130], $Cu_2Zn_{1-x}Fe_xGeSe_4$ [131], $Cu_2Cd_{1-x}Zn_xSnSe_4$ [132] and $Cu_2HgSnSe_{4-x}Te_x$ [107]. In addition, the nanostructuring approach was also employed [133,134]. The enhanced thermoelectric performance can be attributed to the phonon scattering introduced by crystal defects and the increased density of states near the Fermi level, such as $(CuInTe_2)_{0.99}(ZnTe)_{0.01}$ composited with 0.1 wt% TiO_2 nanofiber (zT~1.47 at 823 K) [135], $CuInTe_2$ composited ZnO (zT~1.61 at 823 K) [34].

Distorted diamond-like chalcogenides

There are also numerous diamond-like compounds which crystallize in much distorted structures far from tetragonal, including I_2-IV-VI_3 and $Cu_5Sn_2X_7$ (X=Se, Te) materials. On the one hand, the structural complexity endows them with intrinsically low thermal conductivity [138]; on the other hand, the delocalized p orbitals occupy the VBM, facilitating high mobility and good electrical performance [39,139].

Cu_2SnSe_3 can crystallize into a cubic (F-43m) or monoclinic phase (three types [140]) at room temperature. A high zT of 1.14 at 850 K was achieved *via* In substitution for Sn by Shi *et al.* [39]. Bulk (Ag, In)-co-doped Cu_2SnSe_3 samples were prepared by Li *et al.* [38] *via* a high-pressure combustion synthesis. It was found that Ag doping considerably enhances the Seebeck coefficient. The low electrical conductivity caused by Ag-doping was further compensated by In-doping at Sn site, yielding the maximum $zT = 1.42$ in $Cu_{1.85}Ag_{0.15}Sn_{0.9}In_{0.1}Se_3$ at 823 K. For Cu_2GeSe_3, the electrical conductivity is lower and the Seebeck coefficient is higher due to the large electronegativity of Ge. zT of ~0.5 at 750 K were obtained in Ga-doped Cu_2GeSe_3 samples [144]. Similar results are also found in Cu_2SnS_3 [142,145].

Doping towards higher carrier density is effective to enhance the performance of these Cu_2AX_3 compounds, but it goes the opposite for $Cu_5Sn_2X_7$ (X=Se, Te) with a carrier concentration on the order of 10^{21} cm^{-3}. This is a kind of mixed-valent compound crystallizing in C-centered monoclinic phase with a centrosymmetric space group $C2/m$, being regarded as a super structure of the non-centrosymmetric cubic structure (space group F-43m) as shown in Fig. 13b [141,146].

Tetrahedrite and colusite minerals

With even more complex crystal structures, the diamond-like tetrahedrites and colusites possess 58 and 66 atoms in a crystal cell as shown in Fig. 14a and c, respectively, leading to thermal conductivities smaller than 1 W m^{-1} K^{-1} at room temperature. Notably, the two systems are natural minerals, and both of them crystallize in a cubic structure with space groups of I-43m and P-43n, respectively. Also, they share several common features. Firstly, both of them are very brittle, which is due to the rigid but weak covalent bonds. Secondly, they exhibit a metallic character in electrical transport, i.e., high carrier concentration (on the order of 10^{20} cm^{-3}) and low Seebeck coefficient. This may be related to the high concentration of the intrinsic Cu vacancies. In fact, the carrier concentration for tetrahedrites is too high, and doping or alloying is needed. Thirdly, from the perspective of material processing, it seems difficult to obtain the pure phase for both systems, which may also be related to the weak bonding. Binary and ternary

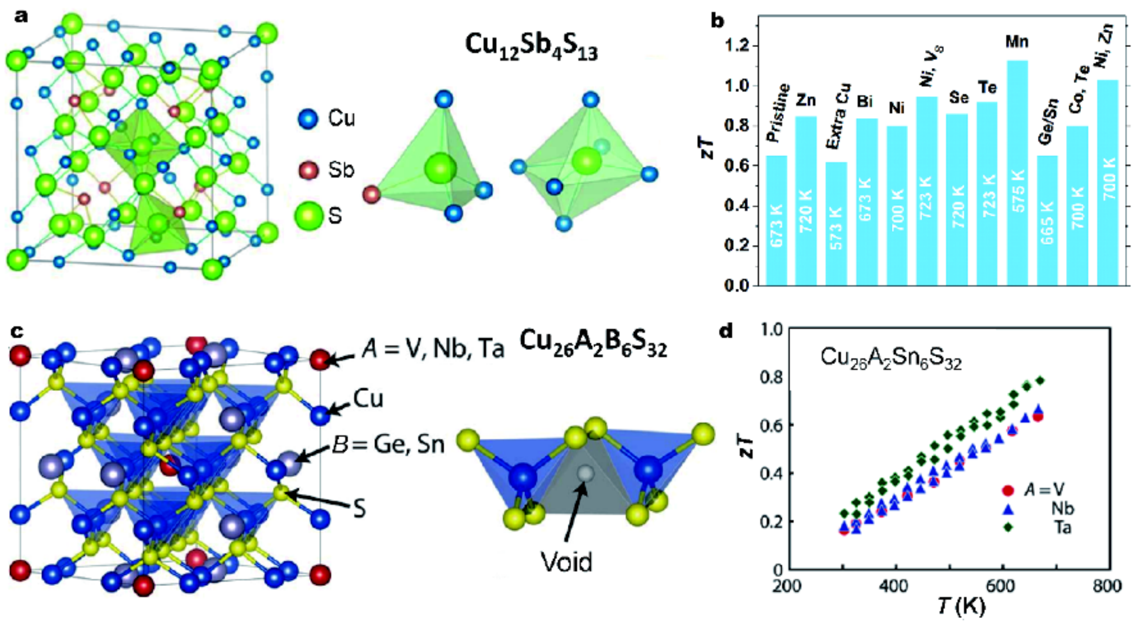

Figure 14 (a) Crystal structure of tetrahedrites, reproduced from Ref. [47], Copyright 2016, American Chemical Society; (b) zT of tetrahedrites [46–49,147–153]; (c) crystal structure and (d) zT of colusites, reproduced from Ref. [43], Copyright 2016, the Royal Society of Chemistry.

impurity phases often exist accompanying with the main phase, which can significantly influence the mechanical and transport properties of the materials.

In 2013, Lu *et al.* [45] reported a zT=0.95 at 720 K in Zn-doped $Cu_{12}Sb_4S_{13}$. Thereafter, various studies on tetrahedrites have been reported with further optimization by doping and alloying as shown in Fig. 14b. A detailed review of the studies on this compound can be found [154]. It is somewhat unexpected that few reports are available on electrical transport analysis probably due to the difficulty in accurate Hall measurement.

Suekuni *et al.* [42,43,155,156] conducted a series of studies on $Cu_{26}A_2B_6S_{32}$ (A=V, Nb, Ta; B=As, Ge, Sn, Sb) colusites. On the one hand, as shown in Fig. 14d, there is no obvious difference in thermoelectric performance among V-, Nb- and Ta-containing compounds, which is consistent with the calculation that VBM (where E_F lies) is composed mostly of Cu-3d and S-3p hybridized orbitals. This hybridization also brings about a large DOS effective mass (4–7m_0) and a decent Seebeck coefficient under a high carrier density. Maximum zT~1.0 was achieved in $Cu_{26}Nb_2Ge_6S_{32}$ at 670 K [44].

OTHER HIGH-PERFORMANCE Cu-BASED CHALCOGENIDES

As shown in Fig. 15, $RCuX_2$ (R = rare earth metals or transition metals, X = S, Se, Te) chalcogenides adopt space groups of $P21/c$, P-3 or P-3m1. Typically, $TmCuTe_2$ with a narrow band gap of 0.23 eV crystallizes in layered structure with a P-3 space group. Lin *et al.* [157] found that Tm ions break the metallic Cu–Cu and the covalent Te–Te bonds interaction. Combined with the intrinsically low thermal conductivity, a high zT of 0.81 was achieved at 745 K. Esmaeili *et al.* [158] reported high electrical resistivity with values ~0.5–500 Ω cm in $RCuX_2$ (R=Gd, Dy, Er) which are larger than the typical high-performance thermoelectric materials by 2–5 orders of magnitude. The thermoelectric performance can be further enhanced by doping at the R site in order to increase the carrier concentration. zT of ~0.75 at 780 K was achieved in $Y_{0.96}Cu_{1.08}Te_2$ owing to the low thermal conductivity with a value of ~0.5 W m^{-1} K^{-1} at 800 K and the optimized electrical transport being resulted from the Y deficiencies [69]. Other rare-earth metal Cu-based chalcogenides such as La_2CuBiS_5 [159] may also be potential thermoelectric materials.

Ba/Cu/X alkali-earth chalcogenides cover a large group of compounds. $BaCu_2Ch_2$ (Ch=S, Se) crystallizes in two stable structures, orthorhombic $BaCu_2S_2$-type and tetragonal $ThCr_2Si_2$-type as shown in Fig. 16 [161]. Kurosaki *et al.* [162] reported a zT of 0.28 at 820 K in potassium-doped β-$BaCu_2S_2$, characterized by layered structure with a space group $I4/mmm$. The decent thermoelectric performance comes from the low thermal conductivity

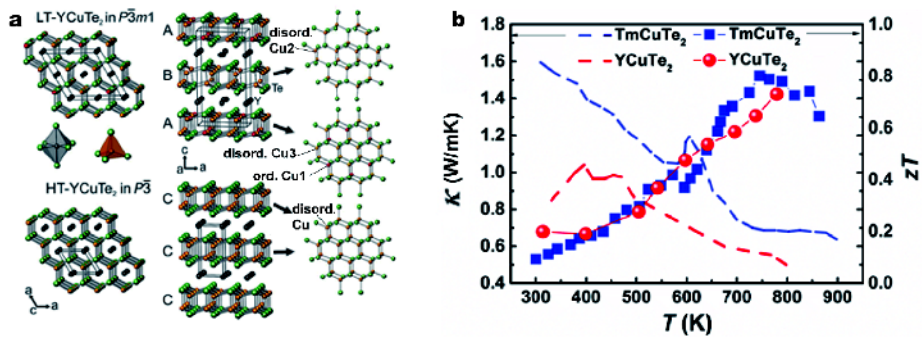

Figure 15 (a) The crystal structure for $YCuTe_2$ in low temperature phase (P-3m1) and high temperature phase (P-3), reproduced from Ref. [69], Copyright 2016, the Royal Society of Chemistry. (b) Thermal conductivity and zT for $YCuTe_2$ and $TmCuTe_2$ [69,157,160].

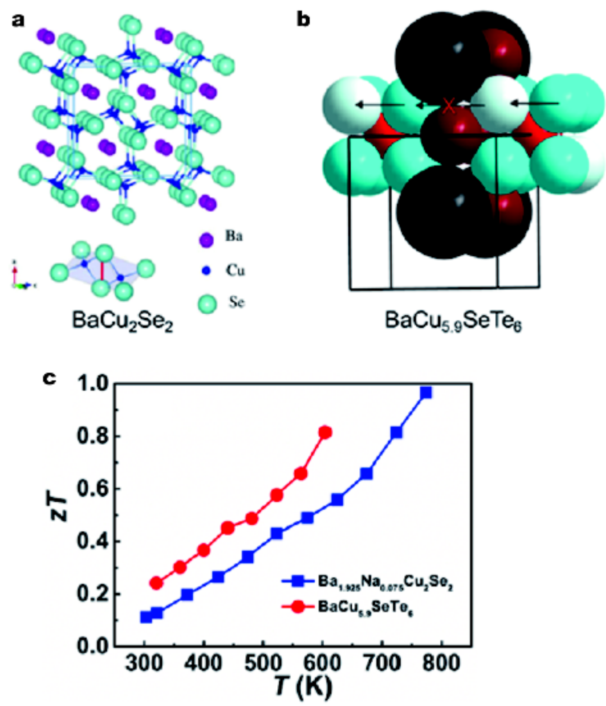

Figure 16 Crystal structure for (a) $BaCu_2Se_2$ (reproduced from Ref. [163], Copyright 2015, the Royal Society of Chemistry) and (b) $BaCu_{5.9}SeTe_6$ (reproduced from Ref. [161], Copyright 2014, American Chemical Society); (c) zT value as a function of the temperature for $Ba_{1.925}Na_{0.075}Cu_2Se_2$ and $BaCu_{5.9}Se(S)Te_6$, respectively [161,163].

(~0.97 W m^{-1} K^{-1}) and the increased carrier concentration by K-doping. The isostructural selenide $Ba_{0.925}Na_{0.075}Cu_2Se_2$ exhibits a higher zT of 1.0 at 773 K [163] (Fig. 16c). Oudah *et al.* [161] reported quaternary $BaCu_{5.9}STe_6$ and $BaCu_{5.9}SeTe_6$ chalcogenides with a zT exceeding 0.8 at around 600 K (Fig. 16c), which was attributed to the low thermal conductivity and the high Seebeck coefficient.

BiCuSeO oxyselenide adopts a layered, ZrCuSiAs-type structure (Fig. 17a), consisting of fluorite $(Bi_2O_2)^{2+}$ layers storing carriers and blocking phonons, and anti-fluorite $(Cu_2Se_2)^{2-}$ layers transferring carriers [164]. Similar to most Cu-based chalcogenides, BiCuSeO shows p-type conductive behavior probably due to the intrinsic Cu vacancies. As a layered material, obvious anisotropy exists in both thermal and electrical transport along in-plane and out-plane directions. The anharmonic bonding and mixed-anion framework in BiCuSeO bring about a low thermal conductivity < 1 W m^{-1} K^{-1}. The zT of BiCuSeO has been increased to ~1.5 through various approaches (see Fig. 17 b–f) including element doping (Mg, Sr, Ca, Ba, Pb at Bi site, Cu vacancies) [51,53,59,165,166], alloying (S, Te) [167], modulation doping [57] and texture treatment [56]. The findings and design methodology of this material are of valuable significance to investigation on similar layered compounds such as SnSe. More details on thermoelectric BiCuSeO can be found in a review article [164].

SUMMARY AND OUTLOOK

In summary, various Cu-based chalcogenides with high abundance and low toxicity have been found to exhibit high zT values well above unity and even about two, which originates from the character of two sublattices and thus the decoupled transport properties. The complex unit cell, distorted or even liquid-like sublattice result in an intrinsically low thermal conductivity while the charge transport network and high band degeneracy guarantee a decent electrical performance.

New and fascinating physical phenomena were brought out along with the emergence of Cu-based chalcogenides, paving new ways for developing high-performance thermoelectric materials. The flowable Cu ions and the liquid-like behavior proposed in Cu_2Se have extended the "PGEC" concept to "PLEC" that has been widely applied

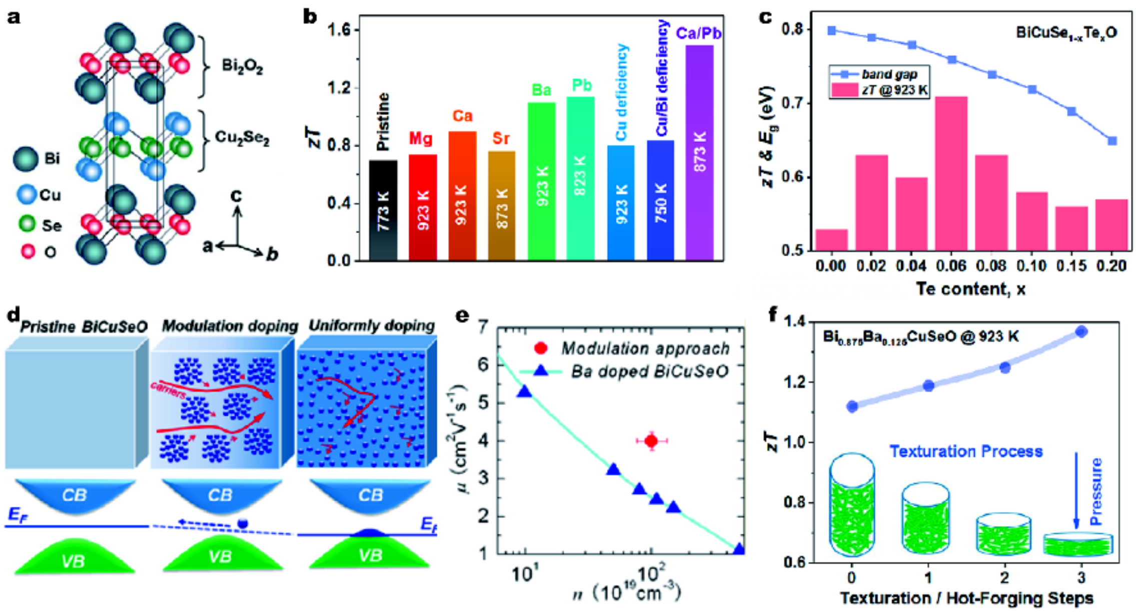

Figure 17 (a) Crystal structure of BiCuSeO, reproduced from Ref. [52] Copyright 2012, the Royal Society of Chemistry; (b) zT values for pristine [52], Bi-site-doped [50,53–55,59,165] and cation-deficient [51,58] BiCuSeO compounds; (c) band gap variation and zT values for BiCuSe$_{1-x}$Te$_x$O [167]; (d) schematic depiction of modulation doping and (e) mobility, reproduced from Ref. [57] Copyright 2014, American Chemical Society; (f) zT as a function of Bi$_{0.875}$Ba$_{0.125}$CuSeO samples before and after hot-forging [56,164].

to other Cu- or Ag-based superionic conductors with extremely low thermal conductivity. The pseudocubic approach has been found effective in screening and optimizing the diamond-like compounds.

There is no escaping the fact that challenges lie ahead for Cu-based chalcogenides operating as high-efficiency thermoelectric materials. Cu ion migration is the key to high zT values of liquid-like compounds but meanwhile seriously hampers the stability and reliability. It is desired to hinder the long-range migration of Cu ions and maintain the short-range motion. For diamond-like Cu-based chalcogenides without ionic migration, the brittle nature brings about the poor machinability, which limits the development of devices. For practical thermoelectric application, it is crucial to step from high-performance materials to high-efficiency devices. In this process, all the factors including the compatibility of materials with electrodes, processability, and stability should be investigated, which are even tougher for new thermoelectric materials. With deeper understanding on the transport mechanisms, availability of more advanced fabrication/processing techniques, we have been trying to solve these problems and it is expected that high-efficiency thermoelectric devices made of Cu-based chalcogenides will come soon.

Received 17 May 2018; accepted 20 June 2018; published online 10 August 2018

1 Nolas G S, Sharp J, Goldsmid H J. Thermoelectrics: Basic Principles and New Materials Developments. Berlin: Springer, 2001
2 Uher C (eds.). Materials Aspect of Thermoelectricity. Boca Raton: CRC Press, 2017
3 Zhu T, Liu Y, Fu C, *et al.* Compromise and synergy in high-efficiency thermoelectric materials. Adv Mater, 2017, 29: 1605884
4 Yang J, Xi L, Qiu W, *et al.* On the tuning of electrical and thermal transport in thermoelectrics: an integrated theory–experiment perspective. NPJ Comput Mater, 2016, 2: 15015
5 Slack G A. New Materials and Performance Limits for Thermoelectric Cooling. In: Rowe D M (eds.). CRC Handbook of Thermoelectrics. Boca Raton: CRC Press, 1995:407-440
6 Snyder GJ, Toberer ES. Complex thermoelectric materials. Nat Mater, 2008, 7: 105–114
7 He J, Tritt TM. Advances in thermoelectric materials research: Looking back and moving forward. Science, 2017, 357: eaak9997
8 Tan G, Zhao LD, Kanatzidis MG. Rationally designing high-performance bulk thermoelectric materials. Chem Rev, 2016, 116: 12123–12149
9 Liu W, Yin K, Zhang Q, *et al.* Eco-friendly high-performance silicide thermoelectric materials. Natl Sci Rev, 2017, 4: 611–626
10 Liu W, Jie Q, Kim HS, *et al.* Current progress and future challenges in thermoelectric power generation: From materials to devices. Acta Mater, 2015, 87: 357–376
11 Li JF, Pan Y, Wu CF, *et al.* Processing of advanced thermoelectric materials. Sci China Technol Sci, 2017, 60: 1347–1364
12 Qiu P, Shi X, Chen L. Cu-based thermoelectric materials. Energy Storage Mater, 2016, 3: 85–97

13 Xiao XX, Xie WJ, Tang XF, *et al.* Phase transition and high temperature thermoelectric properties of copper selenide $Cu_{2-x}Se$ ($0\leq x\leq 0.25$). Chin Phys B, 2011, 20: 087201
14 Liu H, Shi X, Xu F, *et al.* Copper ion liquid-like thermoelectrics. Nat Mater, 2012, 11: 422–425
15 Liu H, Yuan X, Lu P, *et al.* Ultrahigh thermoelectric performance by electron and phonon critical scattering in $Cu_2Se_{1-x}I_x$. Adv Mater, 2013, 25: 6607–6612
16 He Y, Day T, Zhang T, *et al.* High thermoelectric performance in non-toxic earth-abundant copper sulfide. Adv Mater, 2014, 26: 3974–3978
17 He Y, Lu P, Shi X, *et al.* Ultrahigh thermoelectric performance in mosaic crystals. Adv Mater, 2015, 27: 3639–3644
18 He Y, Zhang T, Shi X, *et al.* High thermoelectric performance in copper telluride. NPG Asia Mater, 2015, 7: e210
19 Zhao L, Wang X, Fei FY, *et al.* High thermoelectric and mechanical performance in highly dense $Cu_{2-x}S$ bulks prepared by a melt-solidification technique. J Mater Chem A, 2015, 3: 9432–9437
20 Zhao LL, Wang XL, Wang JY, *et al.* Superior intrinsic thermoelectric performance with zT of 1.8 in single-crystal and melt-quenched highly dense $Cu_{2-x}Se$ bulks. Sci Rep, 2015, 5: 7671
21 Nunna R, Qiu P, Yin M, *et al.* Ultrahigh thermoelectric performance in Cu_2Se-based hybrid materials with highly dispersed molecular CNTs. Energy Environ Sci, 2017, 10: 1928–1935
22 Olvera AA, Moroz NA, Sahoo P, *et al.* Partial indium solubility induces chemical stability and colossal thermoelectric figure of merit in Cu_2Se. Energy Environ Sci, 2017, 10: 1668–1676
23 Zhao K, Blichfeld AB, Chen H, *et al.* Enhanced thermoelectric performance through tuning bonding energy in $Cu_2Se_{1-x}S_x$ liquid-like materials. Chem Mater, 2017, 29: 6367–6377
24 Zhao K, Qiu P, Song Q, *et al.* Ultrahigh thermoelectric performance in $Cu_{2-y}Se_{0.5}S_{0.5}$ liquid-like materials. Mater Today Phys, 2017, 1: 14–23
25 Yang L, Chen ZG, Han G, *et al.* Te-Doped Cu_2Se nanoplates with a high average thermoelectric figure of merit. J Mater Chem A, 2016, 4: 9213–9219
26 Butt S, Xu W, Farooq MU, *et al.* Enhanced thermoelectricity in high-temperature β-phase copper(I) selenides embedded with Cu_2Te nanoclusters. ACS Appl Mater Interfaces, 2016, 8: 15196–15204
27 Gahtori B, Bathula S, Tyagi K, *et al.* Giant enhancement in thermoelectric performance of copper selenide by incorporation of different nanoscale dimensional defect features. Nano Energy, 2015, 13: 36–46
28 Liu ML, Chen IW, Huang FQ, *et al.* Improved thermoelectric properties of Cu-doped quaternary chalcogenides of $Cu_2CdSnSe_4$. Adv Mater, 2009, 21: 3808–3812
29 Shi XY, Huang FQ, Liu ML, *et al.* Thermoelectric properties of tetrahedrally bonded wide-gap stannite compounds $Cu_2ZnSn_{1-x}In_xSe_4$. Appl Phys Lett, 2009, 94: 122103
30 Liu R, Xi L, Liu H, *et al.* Ternary compound $CuInTe_2$: a promising thermoelectric material with diamond-like structure. Chem Commun, 2012, 48: 3818
31 Plirdpring T, Kurosaki K, Kosuga A, *et al.* Chalcopyrite $CuGaTe_2$: A high-efficiency bulk thermoelectric material. Adv Mater, 2012, 24: 3622–3626
32 Zhang J, Liu R, Cheng N, *et al.* High-performance pseudocubic thermoelectric materials from non-cubic chalcopyrite compounds. Adv Mater, 2014, 26: 3848–3853
33 Liu R, Chen H, Zhao K, *et al.* Entropy as a gene-like performance indicator promoting thermoelectric materials. Adv Mater, 2017, 29: 1702712
34 Luo Y, Yang J, Jiang Q, *et al.* Progressive regulation of electrical and thermal transport properties to high-performance $CuInTe_2$ thermoelectric materials. Adv Energy Mater, 2016, 6: 1600007
35 Liu Y, García G, Ortega S, *et al.* Solution-based synthesis and processing of Sn- and Bi-doped Cu_3SbSe_4 nanocrystals, nanomaterials and ring-shaped thermoelectric generators. J Mater Chem A, 2016, 5: 2592–2602
36 Skoug EJ, Cain JD, Morelli DT. High thermoelectric figure of merit in the Cu_3SbSe_4-Cu_3SbS_4 solid solution. Appl Phys Lett, 2011, 98: 261911
37 Liu R, Qin Y, Cheng N, *et al.* Thermoelectric performance of $Cu_{1-x-\delta}Ag_xInTe_2$ diamond-like materials with a pseudocubic crystal structure. Inorg Chem Front, 2016, 3: 1167–1177
38 Li Y, Liu G, Cao T, *et al.* Enhanced thermoelectric properties of Cu_2SnSe_3 by (Ag,In)-Co-doping. Adv Funct Mater, 2016, 26: 6025–6032
39 Shi X, Xi L, Fan J, *et al.* Cu−Se bond network and thermoelectric compounds with complex diamondlike structure. Chem Mater, 2010, 22: 6029–6031
40 Li Y, Liu G, Li J, *et al.* High thermoelectric performance of In-doped Cu_2SnSe_3 prepared by fast combustion synthesis. New J Chem, 2016, 40: 5394–5400
41 Ma R, Liu G, Li J, *et al.* Effect of secondary phases on thermoelectric properties of Cu_2SnSe_3. Ceramics Int, 2017, 43: 7002–7010
42 Suekuni K, Kim FS, Nishiate H, *et al.* High-performance thermoelectric minerals: Colusites $Cu_{26}V_2M_6S_{32}$ (M=Ge, Sn). Appl Phys Lett, 2014, 105: 132107
43 Kikuchi Y, Bouyrie Y, Ohta M, *et al.* Vanadium-free colusites $Cu_{26}A_2Sn_6S_{32}$ (A = Nb, Ta) for environmentally friendly thermoelectrics. J Mater Chem A, 2016, 4: 15207–15214
44 Bouyrie Y, Ohta M, Suekuni K, *et al.* Enhancement in the thermoelectric performance of colusites $Cu_{26}A_2E_6S_{32}$ (A=Nb, Ta; E=Sn, Ge) using E-site non-stoichiometry. J Mater Chem C, 2017, 5: 4174–4184
45 Lu X, Morelli DT, Xia Y, *et al.* High performance thermoelectricity in earth-abundant compounds based on natural mineral tetrahedrites. Adv Energy Mater, 2013, 3: 342–348
46 Heo J, Laurita G, Muir S, *et al.* Enhanced thermoelectric performance of synthetic tetrahedrites. Chem Mater, 2014, 26: 2047–2051
47 Lu X, Morelli DT, Wang Y, *et al.* Phase stability, crystal structure, and thermoelectric properties of $Cu_{12}Sb_4S_{13-x}Se_x$ solid solutions. Chem Mater, 2016, 28: 1781–1786
48 Lu X, Morelli DT, Xia Y, *et al.* Increasing the thermoelectric figure of merit of tetrahedrites by co-doping with nickel and zinc. Chem Mater, 2015, 27: 408–413
49 Prem Kumar DS, Chetty R, Femi OE, *et al.* Thermoelectric properties of Bi doped tetrahedrite. J Elec Mater, 2017, 46: 2616–2622
50 Zhao LD, Berardan D, Pei YL, *et al.* $Bi_{1-x}Sr_xCuSeO$ oxyselenides as promising thermoelectric materials. Appl Phys Lett, 2010, 97: 092118
51 Liu Y, Zhao LD, Liu Y, *et al.* Remarkable enhancement in thermoelectric performance of BiCuSeO by Cu deficiencies. J Am Chem Soc, 2011, 133: 20112–20115
52 Li F, Li JF, Zhao LD, *et al.* Polycrystalline BiCuSeO oxide as a potential thermoelectric material. Energy Environ Sci, 2012, 5:

7188–7195
53 Li J, Sui J, Pei Y, *et al.* A high thermoelectric figure of merit ZT>1 in Ba heavily doped BiCuSeO oxyselenides. Energy Environ Sci, 2012, 5: 8543–8547
54 Lan JL, Zhan B, Liu YC, *et al.* Doping for higher thermoelectric properties in p-type BiCuSeO oxyselenide. Appl Phys Lett, 2013, 102: 123905
55 Pei YL, He J, Li JF, *et al.* High thermoelectric performance of oxyselenides: intrinsically low thermal conductivity of Ca-doped BiCuSeO. NPG Asia Mater, 2013, 5: e47
56 Sui J, Li J, He J, *et al.* Texturation boosts the thermoelectric performance of BiCuSeO oxyselenides. Energy Environ Sci, 2013, 6: 2916–2920
57 Pei YL, Wu H, Wu D, *et al.* High thermoelectric performance realized in a BiCuSeO system by improving carrier mobility through 3D modulation doping. J Am Chem Soc, 2014, 136: 13902–13908
58 Li Z, Xiao C, Fan S, *et al.* Dual vacancies: an effective strategy realizing synergistic optimization of thermoelectric property in BiCuSeO. J Am Chem Soc, 2015, 137: 6587–6593
59 Liu Y, Zhao LD, Zhu Y, *et al.* Synergistically optimizing electrical and thermal transport properties of BiCuSeO *via* a dual-doping approach. Adv Energy Mater, 2016, 6: 1502423
60 Ren GK, Wang SY, Zhu YC, *et al.* Enhancing thermoelectric performance in hierarchically structured BiCuSeO by increasing bond covalency and weakening carrier–phonon coupling. Energy Environ Sci, 2017, 10: 1590–1599
61 Yang D, Su X, Yan Y, *et al.* Manipulating the combustion wave during self-propagating synthesis for high thermoelectric performance of layered oxychalcogenide $Bi_{1-x}Pb_xCuSeO$. Chem Mater, 2016, 28: 4628–4640
62 Toberer ES, Baranowski LL, Dames C. Advances in thermal conductivity. Annu Rev Mater Res, 2012, 42: 179–209
63 Tritt T M. Thermal Conductivity: Theory, Properties and Applications. New York: Plenum, 2004
64 Kittel C. Introduction to Solid State Physics. New York: John Wiley & Sons Inc., 1996
65 Toberer ES, Zevalkink A, Snyder GJ. Phonon engineering through crystal chemistry. J Mater Chem, 2011, 21: 15843–15852
66 Wang X, Qiu P, Zhang T, *et al.* Compound defects and thermoelectric properties in ternary CuAgSe-based materials. J Mater Chem A, 2015, 3: 13662–13670
67 Qiu P, Zhang T, Qiu Y, *et al.* Sulfide bornite thermoelectric material: a natural mineral with ultralow thermal conductivity. Energy Environ Sci, 2014, 7: 4000–4006
68 Weldert KS, Zeier WG, Day TW, *et al.* Thermoelectric transport in Cu_7PSe_6 with high copper ionic mobility. J Am Chem Soc, 2014, 136: 12035–12040
69 Aydemir U, Pöhls JH, Zhu H, *et al.* $YCuTe_2$: a member of a new class of thermoelectric materials with $CuTe_4$-based layered structure. J Mater Chem A, 2016, 4: 2461–2472
70 Bhattacharya S, Basu R, Bhatt R, *et al.* $CuCrSe_2$: a high performance phonon glass and electron crystal thermoelectric material. J Mater Chem A, 2013, 1: 11289–11294
71 Li W, Ibáñez M, Zamani RR, *et al.* $Cu_2HgSnSe_4$ nanoparticles: synthesis and thermoelectric properties. CrystEngComm, 2013, 15: 8966
72 Chetty R, Dadda J, de Boor J, *et al.* The effect of Cu addition on the thermoelectric properties of $Cu_2CdGeSe_4$. Intermetallics, 2015, 57: 156–162
73 Suzumura A, Watanabe M, Nagasako N, *et al.* Improvement in thermoelectric properties of Se-Free Cu_3SbS_4 compound. J Elec Mater, 2014, 43: 2356–2361
74 Li J, Tan Q, Li JF. Synthesis and property evaluation of $CuFeS_{2-x}$ as earth-abundant and environmentally-friendly thermoelectric materials. J Alloys Compd, 2013, 551: 143–149
75 Li W, Lin S, Zhang X, *et al.* Thermoelectric properties of Cu_2SnSe_4 with intrinsic vacancy. Chem Mater, 2016, 28: 6227–6232
76 Vining CB, Laskow W, Hanson JO, *et al.* Thermoelectric properties of pressure-sintered $Si_{0.8}Ge_{0.2}$ thermoelectric alloys. J Appl Phys, 1991, 69: 4333–4340
77 Caillat T, Borshchevsky A, Fleurial JP. Properties of single crystalline semiconducting $CoSb_3$. J Appl Phys, 1996, 80: 4442–4449
78 Liu HL, He Y, Shi X, *et al.* Recent progress in "phonon-liquid" thermoelectric materials. Chin Sci Bull (Chin Ver), 2013, 58: 2603–2608
79 Qiu W, Xi L, Wei P, *et al.* Part-crystalline part-liquid state and rattling-like thermal damping in materials with chemical-bond hierarchy. Proc Natl Acad Sci USA, 2014, 111: 15031–15035
80 Qiu W, Wu L, Ke X, *et al.* Diverse lattice dynamics in ternary Cu-Sb-Se compounds. Sci Rep, 2015, 5: 13643
81 Li B, Wang H, Kawakita Y, *et al.* Liquid-like thermal conduction in intercalated layered crystalline solids. Nat Mater, 2018, 17: 226–230
82 Voneshen DJ, Walker HC, Refson K, *et al.* Hopping time scales and the phonon-liquid electron-crystal picture in thermoelectric copper selenide. Phys Rev Lett, 2017, 118: 145901
83 Skoug EJ, Morelli DT. Role of lone-pair electrons in producing minimum thermal conductivity in nitrogen-group chalcogenide compounds. Phys Rev Lett, 2011, 107: 235901
84 Sun Y, Xi L, Yang J, *et al.* The "electron crystal" behavior in copper chalcogenides Cu_2X (X = Se, S). J Mater Chem A, 2017, 5: 5098–5105
85 Zou D, Xie S, Liu Y, *et al.* Electronic structures and thermoelectric properties of layered BiCuOCh oxychalcogenides (Ch = S, Se and Te): first-principles calculations. J Mater Chem A, 2013, 1: 8888–8896
86 Do D, Ozolins V, Mahanti SD, *et al.* Physics of bandgap formation in Cu–Sb–Se based novel thermoelectrics: the role of Sb valency and Cu d levels. J Phys-Condens Matter, 2012, 24: 415502
87 Qin Y, Qiu P, Liu R, *et al.* Optimized thermoelectric properties in pseudocubic diamond-like $CuGaTe_2$ compounds. J Mater Chem A, 2016, 4: 1277–1289
88 Song Q, Qiu P, Hao F, *et al.* Quaternary pseudocubic $Cu_2TMSnSe_4$ (TM = Mn, Fe, Co) chalcopyrite thermoelectric materials. Adv Electron Mater, 2016, 2: 1600312
89 Zeier WG, Zevalkink A, Gibbs ZM, *et al.* Thinking like a chemist: intuition in thermoelectric materials. Angew Chem Int Ed, 2016, 55: 6826–6841
90 Zhao K, Blichfeld AB, Eikeland E, *et al.* Extremely low thermal conductivity and high thermoelectric performance in liquid-like $Cu_2Se_{1-x}S_x$ polymorphic materials. J Mater Chem A, 2017, 5: 18148–18156
91 Zhao K, Zhu C, Qiu P, *et al.* High thermoelectric performance and low thermal conductivity in $Cu_{2-y}S_{1/3}Se_{1/3}Te_{1/3}$ liquid-like materials with nanoscale mosaic structures. Nano Energy, 2017, 42: 43–50
92 Xie Y. Mosaic crystals leading a new route to achieve ultrahigh thermoelectric performance. Sci China Mater, 2015, 58: 431–432
93 Ge ZH, Liu X, Feng D, *et al.* High-performance thermoelectricity

in nanostructured earth-abundant copper sulfides bulk materials. Adv Energy Mater, 2016, 6: 1600607
94 Jiang B, Qiu P, Eikeland E, *et al.* Cu_8GeSe_6-based thermoelectric materials with an argyrodite structure. J Mater Chem C, 2017, 5: 943–952
95 Qiu PF, Wang XB, Zhang TS, *et al.* Thermoelectric properties of Te-doped ternary CuAgSe compounds. J Mater Chem A, 2015, 3: 22454–22461
96 Bhattacharya S, Bohra A, Basu R, *et al.* High thermoelectric performance of $(AgCrSe_2)_{0.5}(CuCrSe_2)_{0.5}$ nano-composites having all-scale natural hierarchical architectures. J Mater Chem A, 2014, 2: 17122–17129
97 Hwang JY, Mun HA, Kim SI, *et al.* Effects of doping on transport properties in Cu–Bi–Se-based thermoelectric materials. Inorg Chem, 2014, 53: 12732–12738
98 Ishiwata S, Shiomi Y, Lee JS, *et al.* Extremely high electron mobility in a phonon-glass semimetal. Nat Mater, 2013, 12: 512–517
99 Han CG, Zhang BP, Ge ZH, *et al.* Thermoelectric properties of p-type semiconductors copper chromium disulfide $CuCrS_{2+x}$. J Mater Sci, 2013, 48: 4081–4087
100 Gągor A, Pietraszko A, Kaynts D. Diffusion paths formation for Cu^+ ions in superionic Cu_6PS_5I single crystals studied in terms of structural phase transition. J Solid State Chem, 2005, 178: 3366–3375
101 Miyatani S, Suzuki Y. On the electric conductivity of cuprous sulfide: experiment. J Phys Soc Jpn, 1953, 8: 680–681
102 Ema Y. Cu electromigration effect on $Cu_{2-x}Se$ film properties. Jpn J Appl Phys, 1990, 29: 2098–2102
103 Bailey TP, Hui S, Xie H, *et al.* Enhanced *ZT* and attempts to chemically stabilize Cu_2Se *via* Sn doping. J Mater Chem A, 2016, 4: 17225–17235
104 Qiu P, Agne MT, Liu Y, *et al.* Suppression of atom motion and metal deposition in mixed ionic/electronic conductors. Nat Commun, 2018, 9: 2910
105 Tang H, Sun FH, Dong JF, *et al.* Graphene network in copper sulfide leading to enhanced thermoelectric properties and thermal stability. Nano Energy, 2018, 49: 267–273
106 Li W, Ibáñez M, Cadavid D, *et al.* Colloidal synthesis and functional properties of quaternary Cu-based semiconductors: $Cu_2HgGeSe_4$. J Nanopart Res, 2014, 16: 2297
107 Navrátil J, Kucek V, Plecháček T, *et al.* Thermoelectric properties of $Cu_2HgSnSe_4$-$Cu_2HgSnTe_4$ solid solution. J Elec Materi, 2014, 43: 3719–3725
108 Pavan Kumar V, Guilmeau E, Raveau B, *et al.* A new wide band gap thermoelectric quaternary selenide $Cu_2MgSnSe_4$. J Appl Phys, 2015, 118: 155101
109 Ibáñez M, Zamani R, LaLonde A, *et al.* $Cu_2ZnGeSe_4$ nanocrystals: synthesis and thermoelectric properties. J Am Chem Soc, 2012, 134: 4060–4063
110 Doverspike K, Dwight K, Wold A. Preparation and characterization of copper zinc germanium sulfide selenide ($Cu_2ZnGeS_{4-y}Se_y$). Chem Mater, 1990, 2: 194–197
111 Xie H, Su X, Zheng G, *et al.* The role of Zn in chalcopyrite $CuFeS_2$: enhanced thermoelectric properties of $Cu_{1-x}Zn_xFeS_2$ with *in situ* nanoprecipitates. Adv Energy Mater, 2016, 7: 1601299
112 Li D, Li R, Qin XY, *et al.* Co-precipitation synthesis of Sn and/or S doped nanostructured $Cu_3Sb_{1-x}Sn_xSe_{4-y}S_y$ with a high thermoelectric performance. CrystEngComm, 2013, 15: 7166–7170
113 Wei TR, Wang H, Gibbs ZM, *et al.* Thermoelectric properties of Sn-doped p-type Cu_3SbSe_4: a compound with large effective mass and small band gap. J Mater Chem A, 2014, 2: 13527–13533
114 Cheng N, Liu R, Bai S, *et al.* Enhanced thermoelectric performance in Cd doped $CuInTe_2$ compounds. J Appl Phys, 2014, 115: 163705
115 Zhang J, Qin X, Li D, *et al.* Enhanced thermoelectric properties of Ag-doped compounds $CuAg_xGa_{1-x}Te_2$ ($0\leq x\leq 0.05$). J Alloys Compd, 2014, 586: 285–288
116 Kucek V, Drasar C, Kasparova J, *et al.* High-temperature thermoelectric properties of Hg-doped $CuInTe_2$. J Appl Phys, 2015, 118: 125105
117 Kucek V, Drasar C, Navratil J, *et al.* Thermoelectric properties of Ni-doped $CuInTe_2$. J Phys Chem Solids, 2015, 83: 18–23
118 Shen J, Chen Z, lin S, *et al.* Single parabolic band behavior of thermoelectric p-type $CuGaTe_2$. J Mater Chem C, 2016, 4: 209–214
119 Li Y, Zhang T, Qin Y, *et al.* Thermoelectric transport properties of diamond-like $Cu_{1-x}Fe_{1+x}S_2$ tetrahedral compounds. J Appl Phys, 2014, 116: 203705
120 Li XY, Li D, Xin HX, *et al.* Effects of bismuth doping on the thermoelectric properties of Cu_3SbSe_4 at moderate temperatures. J Alloys Compd, 2013, 561: 105–108
121 Yang C, Huang F, Wu L, *et al.* New stannite-like p-type thermoelectric material Cu_3SbSe_4. J Phys D-Appl Phys, 2011, 44: 295404
122 Skoug EJ, Cain JD, Majsztrik P, *et al.* Doping effects on the thermoelectric properties of Cu_3SbSe_4. Sci Adv Mat, 2011, 3: 602–606
123 Chetty R, Bali A, Mallik RC. Thermoelectric properties of indium doped $Cu_2CdSnSe_4$. Intermetallics, 2016, 72: 17–24
124 Kosuga A, Higashine R, Plirdpring T, *et al.* Effects of the defects on the thermoelectric properties of Cu–In–Te chalcopyrite-related compounds. Jpn J Appl Phys, 2012, 51: 121803
125 Wei TR, Li F, Li JF. Enhanced thermoelectric performance of nonstoichiometric compounds $Cu_{3-x}SbSe_4$ by Cu deficiencies. J Elec Mater, 2014, 43: 2229–2238
126 Goto Y, Naito F, Sato R, *et al.* Enhanced thermoelectric figure of merit in Stannite–Kuramite solid solutions $Cu_{2+x}Fe_{1-x}SnS_{4-y}$ (x= 0–1) with anisotropy lowering. Inorg Chem, 2013, 52: 9861–9866
127 Zeier WG, Heinrich CP, Day T, *et al.* Bond strength dependent superionic phase transformation in the solid solution series $Cu_2ZnGeSe_{4-x}S_x$. J Mater Chem A, 2014, 2: 1790–1794
128 Berman R. Thermal Conduction in Solids. Oxford: Clarendon Press, 1976
129 Li Y, Meng Q, Deng Y, *et al.* High thermoelectric performance of solid solutions $CuGa_{1-x}In_xTe_2$ ($x = 0$–1.0). Appl Phys Lett, 2012, 100: 231903
130 Skoug EJ, Cain JD, Morelli DT, *et al.* Lattice thermal conductivity of the Cu_3SbSe_4-Cu_3SbS_4 solid solution. J Appl Phys, 2011, 110: 023501
131 Zeier WG, Pei Y, Pomrehn G, *et al.* Phonon scattering through a local anisotropic structural disorder in the thermoelectric solid solution $Cu_2Zn_{1-x}Fe_xGeSe_4$. J Am Chem Soc, 2013, 135: 726–732
132 Liu FS, Wang B, Ao WQ, *et al.* Crystal structure and thermoelectric properties of $Cu_2Cd_{1-x}Zn_xSnSe_4$ solid solutions. Intermetallics, 2014, 55: 15–21
133 Li Z, Xiao C, Zhu H, *et al.* Defect chemistry for thermoelectric materials. J Am Chem Soc, 2016, 138: 14810–14819
134 Chen H, Yang C, Liu H, *et al.* Thermoelectric properties of $CuInTe_2$/graphene composites. CrystEngComm, 2013, 15: 6648–6651

135 Luo Y, Yang J, Jiang Q, *et al.* Large enhancement of thermoelectric performance of $CuInTe_2$ *via* a synergistic strategy of point defects and microstructure engineering. Nano Energy, 2015, 18: 37–46
136 Dong Y, Wang H, Nolas GS. Synthesis, crystal structure, and high temperature transport properties of p-type $Cu_2Zn_{1-x}Fe_xSnSe_4$. Inorg Chem, 2013, 52: 14364–14367
137 Dong Y, Wang H, Nolas GS. Synthesis and thermoelectric properties of Cu excess $Cu_2ZnSnSe_4$. Phys Status Solidi RRL, 2014, 8: 61–64
138 Cho JY, Shi X, Salvador JR, *et al.* Thermoelectric properties of ternary diamondlike semiconductors $Cu_2Ge_{1+x}Se_3$. J Appl Phys, 2010, 108: 073713
139 Xi L, Zhang YB, Shi XY, *et al.* Chemical bonding, conductive network, and thermoelectric performance of the ternary semiconductors Cu_2SnX_3 (X=Se, S) from first principles. Phys Rev B, 2012, 86: 155201
140 Fan J, Carrillo-Cabrera W, Akselrud L, *et al.* New monoclinic phase at the composition Cu_2SnSe_3 and its thermoelectric properties. Inorg Chem, 2013, 52: 11067–11074
141 Fan J, Carrillo-Cabrera W, Antonyshyn I, *et al.* Crystal structure and physical properties of ternary phases around the composition $Cu_5Sn_2Se_7$ with tetrahedral coordination of atoms. Chem Mater, 2014, 26: 5244–5251
142 Tan Q, Sun W, Li Z, *et al.* Enhanced thermoelectric properties of earth-abundant Cu_2SnS_3 *via* in doping effect. J Alloys Compd, 2016, 672: 558–563
143 Huang T, Yan Y, Peng K, *et al.* Enhanced thermoelectric performance in copper-deficient Cu_2GeSe_3. J Alloys Compd, 2017, 723: 708–713
144 Cho JY, Shi X, Salvador JR, *et al.* Thermoelectric properties and investigations of low thermal conductivity in Ga-doped Cu_2GeSe_3. Phys Rev B, 2011, 84: 085207
145 Shen Y, Li C, Huang R, *et al.* Eco-friendly p-type Cu_2SnS_3 thermoelectric material: crystal structure and transport properties. Sci Rep, 2016, 6: 32501
146 Adhikary A, Mohapatra S, Lee SH, *et al.* Metallic ternary telluride with sphalerite superstructure. Inorg Chem, 2016, 55: 2114–2122
147 Vaqueiro P, Guélou G, Kaltzoglou A, *et al.* The influence of mobile copper ions on the glass-like thermal conductivity of copper-rich tetrahedrites. Chem Mater, 2017, 29: 4080–4090
148 Sun FH, Wu CF, Li Z, *et al.* Powder metallurgically synthesized $Cu_{12}Sb_4S_{13}$ tetrahedrites: phase transition and high thermoelectricity. RSC Adv, 2017, 7: 18909–18916
149 Barbier T, Lemoine P, Gascoin S, *et al.* Structural stability of the synthetic thermoelectric ternary and nickel-substituted tetrahedrite phases. J Alloys Compd, 2015, 634: 253–262
150 Lu X, Morelli D. The effect of Te substitution for Sb on thermoelectric properties of tetrahedrite. J Elec Materi, 2014, 43: 1983–1987
151 Kosaka Y, Suekuni K, Hashikuni K, *et al.* Effects of Ge and Sn substitution on the metal–semiconductor transition and thermoelectric properties of $Cu_{12}Sb_4S_{13}$ tetrahedrite. Phys Chem Chem Phys, 2017, 19: 8874–8879
152 Bouyrie Y, Sassi S, Candolfi C, *et al.* Thermoelectric properties of double-substituted tetrahedrites $Cu_{12-x}Co_xSb_{4-y}Te_yS_{13}$. Dalton Trans, 2016, 45: 7294–7302
153 Sun FH, Dong J, Dey S, *et al.* Enhanced thermoelectric performance of $Cu_{12}Sb_4S_{13-\delta}$ tetrahedrite *via* nickel doping. Sci China Mater, 2018, 61: 1209–1217
154 Chetty R, Bali A, Mallik RC. Tetrahedrites as thermoelectric materials: an overview. J Mater Chem C, 2015, 3: 12364–12378
155 Kim FS, Suekuni K, Nishiate H, *et al.* Tuning the charge carrier density in the thermoelectric colusite. J Appl Phys, 2016, 119: 175105
156 Suekuni K, Tsuruta K, Kunii M, *et al.* High-performance thermoelectric mineral $Cu_{12-x}Ni_xSb_4S_{13}$ tetrahedrite. J Appl Phys, 2013, 113: 043712
157 Lin H, Chen H, Shen JN, *et al.* Chemical modification and energetically favorable atomic disorder of a layered thermoelectric material $TmCuTe_2$ leading to high performance. Chem Eur J, 2014, 20: 15401–15408
158 Esmaeili M, Tseng YC, Mozharivskyj Y. Thermoelectric properties, crystal and electronic structure of semiconducting $RECuSe_2$ (RE=Pr, Sm, Gd, Dy and Er). J Alloys Compd, 2014, 610: 555–560
159 Yang G, Yao Y, Ma D. Structural, electronic, and thermoelectric properties of La_2CuBiS_5. Sci China Mater, 2017, 60: 151–158
160 Gulay LD, Daszkiewicz M, Shemet VY. Crystal structure of $\sim RCu_3S_3$ and $\sim RCuTe_2$ (R=Gd–Lu) compounds. J Solid State Chem, 2012, 186: 142–148
161 Oudah M, Kleinke KM, Kleinke H. Thermoelectric properties of the quaternary chalcogenides $BaCu_{5.9}STe_6$ and $BaCu_{5.9}SeTe_6$. Inorg Chem, 2014, 54: 845–849
162 Kurosaki K, Uneda H, Muta H, *et al.* Thermoelectric properties of potassium-doped β-$BaCu_2S_2$ with natural superlattice structure. J Appl Phys, 2005, 97: 053705
163 Li J, Zhao LD, Sui J, *et al.* $BaCu_2Se_2$ based compounds as promising thermoelectric materials. Dalton Trans, 2015, 44: 2285–2293
164 Zhao LD, He J, Berardan D, *et al.* BiCuSeO oxyselenides: new promising thermoelectric materials. Energy Environ Sci, 2014, 7: 2900–2924
165 Lan JL, Liu YC, Zhan B, *et al.* Enhanced thermoelectric properties of Pb-doped BiCuSeO ceramics. Adv Mater, 2013, 25: 5086–5090
166 Li F, Wei TR, Kang F, *et al.* Enhanced thermoelectric performance of Ca-doped BiCuSeO in a wide temperature range. J Mater Chem A, 2013, 1: 11942–11949
167 Liu Y, Lan J, Xu W, *et al.* Enhanced thermoelectric performance of a BiCuSeO system *via* band gap tuning. Chem Commun, 2013, 49: 8075–8077

Acknowledgements This review is supported by the National Key Research and Development Program of China (2018YFB0703600), the National Natural Science Foundation of China (51625205), the Key Research Program of Chinese Academy of Sciences (KFZD-SW-421), Program of Shanghai Subject Chief Scientist (16XD1403900), Youth Innovation Promotion Association, CAS (2016232) and Shanghai Sailing Program (18YF1426700).

Author contributions Shi X and Chen L designed the topic and framework of this review; Wei TR, Qin Y and Qiu P collected and organized the data; Wei TR and Qin Y wrote the review with the support from Qiu P, Shi X and Chen L. All authors contributed to the general discussion.

Conflict of interest The authors declare no conflict of interest.

Tian-Ran Wei is an assistant professor at Shanghai Institute of Ceramics, Chinese Academy of Sciences (SICCAS). He obtained his PhD degree in materials science and engineering from Tsinghua University in 2017. His current research focuses on advanced thermoelectric materials and the underlying transport mechanisms.

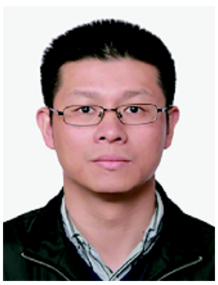

Xun Shi is a Professor in SICCAS, China. He received his BSc (2000) in Tsinghua University and PhD (2005) in the University of Chinese Academy of Sciences. He worked at the University of Michigan (USA) as a postdoctor from 2007 to 2009. Then he joined the R&D center in General Motors. At 2010, he came back SICCAS. His current research focuses on advanced thermoelectric materials.

铜基硫族化合物热电材料

魏天然[1], 覃玉婷[1,2], 邓婷婷[1,2], 宋庆峰[1,2], 江彬彬[1,2], 刘睿恒[1], 仇鹏飞[1], 史迅[1*], 陈立东[1]

摘要 铜基硫族化合物因其高性能、可调的输运性质、高丰度和低毒性，被认为是很有前景的新型热电材料，引起了研究者的广泛关注. 本文总结了近年来铜基热电材料的研究进展，包括类金刚石结构材料、声子液体二元及多元化合物等. 本文首先总体介绍了两套亚晶格的基本特征及其对热学、电学性质的影响: 一方面，复杂晶体结构和无序、甚至液态化的亚晶格导致极低的热导率; 另一方面，刚性亚晶格构成电荷传输通道，保证了较高的电学性能. 然后，本文针对特定的几类材料体系，详细介绍了其典型结构特征与“结构-性能”构效关系，以及掺杂、固溶、能带结构调控和纳米结构设计等多尺度优化手段. 最后，本文从材料研发和器件研制的角度评述了铜基硫族化合物作为热电材料的应用前景及相关进展.

